

# Stability of Molten Core Materials

Layne Pincock  
Wendell Hintze

January 2013



The INL is a U.S. Department of Energy National Laboratory  
operated by Battelle Energy Alliance

# **Stability of Molten Core Materials**

**Layne Pincock**  
**Wendell Hintze**

**January 2013**

**Idaho National Laboratory**  
**Idaho Falls, Idaho 83415**

**<http://www.inl.gov>**

**Prepared for the**  
**Central Research Institute of Electric Power Industry**  
**WFO Project #12902**  
**and for the**  
**U.S. Department of Energy**  
**Under DOE Idaho Operations Office**  
**Contract DE-AC07-05ID14517**

#### **DISCLAIMER**

This information was prepared as an account of work sponsored by an agency of the U.S. Government. Neither the U.S. Government nor any agency thereof, nor any of their employees, makes any warranty, expressed or implied, or assumes any legal liability or responsibility for the accuracy, completeness, or usefulness, of any information, apparatus, product, or process disclosed, or represents that its use would not infringe privately owned rights. References herein to any specific commercial product, process, or service by trade name, trade mark, manufacturer, or otherwise, does not necessarily constitute or imply its endorsement, recommendation, or favoring by the U.S. Government or any agency thereof. The views and opinions of authors expressed herein do not necessarily state or reflect those of the U.S. Government or any agency thereof.



# Stability of Molten Core Materials

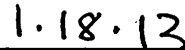
INL/EXT-12-27136  
Revision 1

January 2013

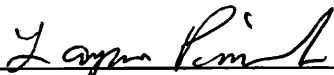
Approved by:



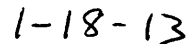
Sandra Birk  
Manager, Nuclear Materials Disposition & Engineering



Date



Layne Pincock  
Nuclear Materials Disposition & Engineering



Date



## **ABSTRACT**

The purpose of this report is to document a literature and data search for data and information pertaining to the stability of nuclear reactor molten core materials. This includes data and analysis from TMI-2 fuel and INL's LOFT (Loss of Fluid Test) reactor project and other sources.





## CONTENTS

ABSTRACT.....	v
1. INTRODUCTION .....	1
2. TMI-2 BACKGROUND .....	1
3. CANISTER DESCRIPTIONS .....	2
3.1 Fuel Canister .....	2
3.2 Knockout Canister.....	3
3.3 Filter Canister Description .....	5
3.4 TMI-2 Shipments .....	6
3.5 Leaching Data .....	11
3.6 Uranium and Plutonium Estimates.....	20
3.7 Discussion of Leachability.....	20
3.8 Corrosivity of Solutions .....	21
4. LOSS OF FLUID TEST FACILITY (LOFT) DATA .....	21
4.1 Leaching Data .....	22
4.2 Metallography .....	22
5. OTHER DATA.....	23
5.1 IAEA Leach Test Results.....	24
5.2 Leaching of Irradiated LWR Fuel in a Simulated Post-Accident Environment.....	24
6. REFERENCES .....	25
Appendix A Sampling/Analytical Methods.....	1

## FIGURES

Figure 1. The TMI-2 canister designs.....	1
Figure 2. Fuel canister bulkhead cross section. ....	2
Figure 3. Fuel canister cross section. ....	3
Figure 4. Knockout canister cross section at mid-plane. ....	4
Figure 5. Knockout canister ports and internals.....	4
Figure 6. Filter canister cross section at mid-plane.....	5
Figure 7. Filter module. ....	6
Figure 8.Canister loading data for Canister D-180. ....	8
Figure 9.Canister loading data for Canister D-188. ....	9
Figure 10. Canister loading data for Canister D-330.....	10
Figure 11. Sample results plot for Canister D-180. ....	14

Figure 12. Sample results plot for Canister D-188. ....	15
Figure 13. Sample results plot for Canister D-330. ....	16
Figure 14. Sample results plot for Canister F-462. ....	17
Figure 15. Sample results plot for Canister K-506. ....	18
Figure 16. Maximum and minimum results plot.....	19

## TABLES

Table 1. Sample results for materials in canister water. ....	12
Table 2. Sample results for radionuclides in canister water (as of December 1995).....	13
Table 3. Canister water radioactivity (as of December 1995).....	13
Table 4. Canister data (for shipments to INL). ....	19
Table 5. Calculated average (of the maximum) leach rates for all five canister sample results. ....	21
Table 6. Cumulative release fractions of the damaged fuel to the blowdown suppression tank (BST). ....	23
Table 8. IAEA leach rates for 28,000 MWd/MTU spent fuel at 25°C at 467 days (g/cm <sup>2</sup> -day).....	24

# Stability of Molten Core Materials

## 1. INTRODUCTION

In March of 2011 a massive earthquake hit Japan along with a very large tsunami, causing widespread damage in the region. Because backup power for cooling was disrupted at the Fukushima Daiichi Nuclear Power Plant, the fuel in Units 1–3 experienced melting before cooling water circulation could be restored. It is important for the Fukushima cleanup and recovery effort to understand the behavior of this damaged fuel in water over time. Pertinent data from Three Mile Island Unit 2 (TMI-2) and other sources could be used to better understand this behavior.

## 2. TMI-2 BACKGROUND

The three types of canisters used to contain debris from TMI-2 were fuel canisters, knockout canisters, and filter canisters (see Figure 1). These canisters were all constructed of 304L stainless steel. The fuel canisters have a square shroud of stainless steel surrounded by a stainless steel enclosed sheet of Boral. Low density concrete (Licon) fills the void between the shroud and the edge of the canister. The fuel canisters hold large pieces of core debris. The knockout canisters hold fine fuel particles and debris ranging in size from 140  $\mu\text{m}$  up to whole fuel pellets. The filter canisters contain filters that contain particulates in the range of 0.5 to 800  $\mu\text{m}$ . All of the canisters were filled under water in the reactor vessel, which had been flooded with water containing boron, for criticality control.

A total of 342 TMI-2 canisters were used, which breaks down to 268 fuel canisters, 12 knockout canisters, and 62 filter canisters. Each canister was given a unique identifier as follows: fuel canisters start with D (for debris; e.g., D-301), knockout canisters start with K (e.g., K-501), and filter canisters start with F (e.g., F-401).

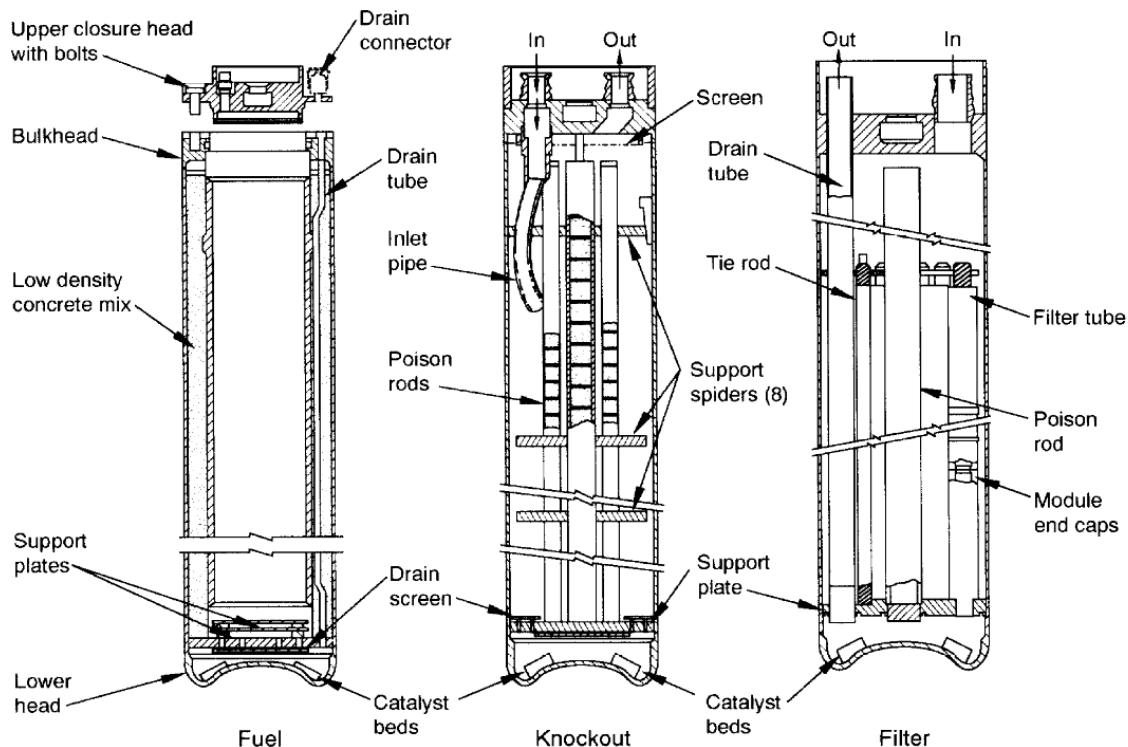


Figure 1. The TMI-2 canister designs.

### 3. CANISTER DESCRIPTIONS

#### 3.1 Fuel Canister

The fuel canister consisted of a cylindrical pressure vessel with a flat upper closure head as shown in Figure 2. It used the same generic outer shell as the other canisters, except for its removable upper closure head, which was attached with bolts. Within the shell, a full length square shroud formed the internal cavity. This shroud was supported at the top by a bulkhead that mates with the upper closure head. The shroud and debris rested on a support plate welded to the shell. The support plate had impact plates attached to help absorb canister drop loads and payload drop loads.

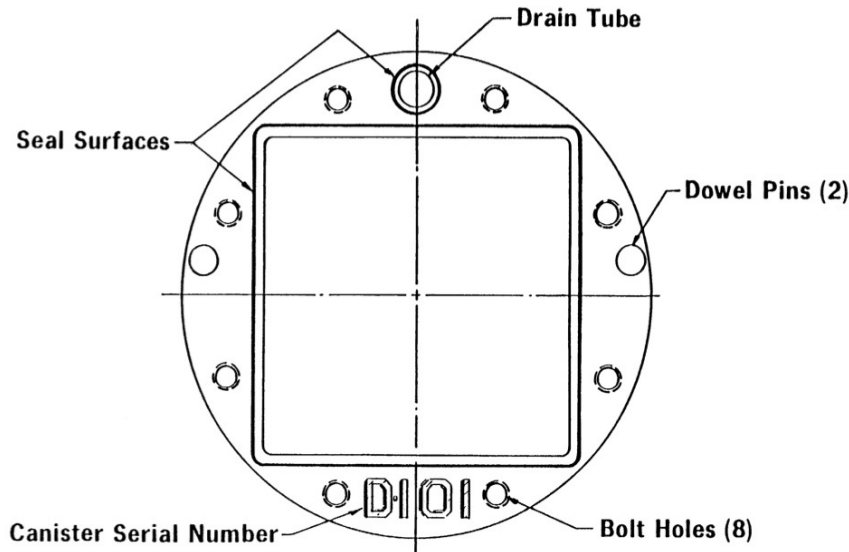


Figure 2. Fuel canister bulkhead cross section.

The canister's square-within-a-circle configuration is evident in the design of the upper bulkhead as shown in Figure 3. Tapped to accept the bolts attaching the upper closure head, the bulkhead's top surface also interfaces with the seal-ring in the closure head to seal the canister. A drain tube is welded into a machined hole in the bulkhead. Two nonsymmetrical locating pins on the upper surface ensure the closure head is installed in the correct orientation. Circular indentations in the sides of the square opening provide an interface with the canister lifting tool when the closure head is not installed.

The shroud assembly consisted of a pair of concentric square stainless-steel tubes, seal-welded to completely encapsulate four sheets of Boral (a neutron absorbing material). Across the diagonal, the shroud is dimensionally only slightly smaller than the outer shell's inner diameter. This fit-up gives the shroud support at the corners for any lateral loads. A thick walled spacer tube is welded on the outside of each flat side to prevent large deformations in the square configuration in lateral loading conditions. The inner cavity of the shroud, a 9.00 inch square, encompasses the fuel assembly's square envelope of 8.54 inches. Based on refueling experience, these canister dimensions ensured that partial fuel assemblies meeting the cross-section dimensions of normally irradiated PWR fuel could be inserted into the canister.

The upper closure head is attached to the bulkhead by eight equally spaced self-locking three-quarter-inch diameter bolts. These bolts were sized for the pressure loads and postulated impact force from shifting of the canister contents during a shipping accident. All the bolts are captured within the closure assembly and handled as an assembly.

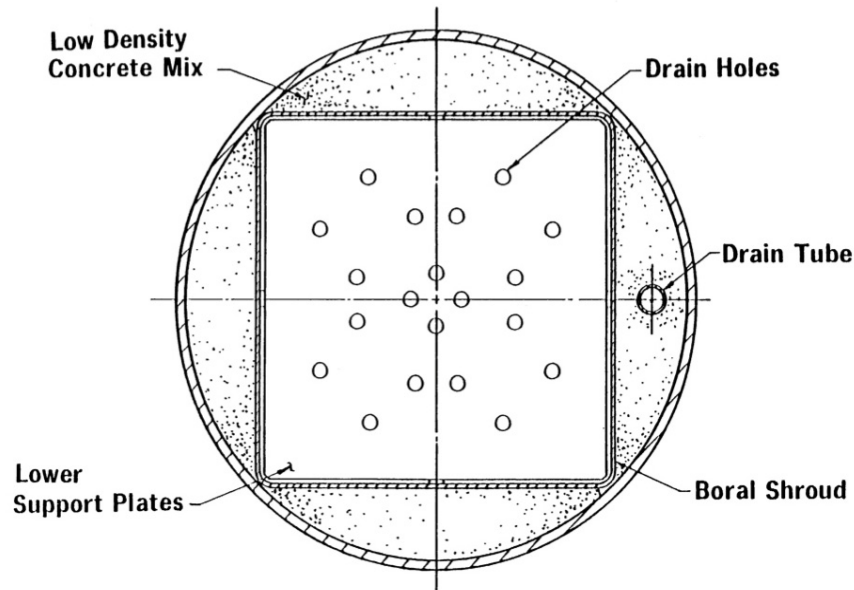


Figure 3. Fuel canister cross section.

Alignment pin holes and the drain tube hole match the corresponding items in the bulkhead. Grooves for the two metallic seal-rings that go around the square opening and drain line are machined into the bottom side of the head. These seal-rings are attached to the upper head using small screws and spring clips that can be replaced remotely.

The regions between the Boral shroud and the outer pressure vessel are filled with LICON, a low density mixture of hydraulic refractory cement and glass beads.

### 3.2 Knockout Canister

The knockout canister shown in Figure 4 (part of the fines/debris vacuum system) was designed to hold debris ranging in size from 140 microns to whole fuel pellets. The influent came directly from the defueling vacuum system inside the reactor, while the outlet flow went to a filter canister for further treatment. Flow fittings were Hansen type and were capped or plugged after use similar to the filter canister. Externally, the knockout canister was very similar to the other canisters using the same outer shell design. It also incorporated the same handling tool interface. The knockout canister internals design was the result of a joint effort between B&W and Westinghouse. B&W's scope of supply was the structural design and the criticality analysis, while Westinghouse was responsible for the flow/debris separation performance.

The internals module for the knockout canister was supported from a lower header welded to the outer shell positioned by chock blocks at the upper header as shown in Figure 5. An array of four outer absorber rods around a central absorber rod was located in the canister for criticality control. The four outer rods had 1.315 in. outer diameter tubes filled with neutron absorbing material, vibrapacked B<sub>4</sub>C powder. The central absorber rod was similar to the one used in the filter canister. It was comprised of a 2.075 in. outer diameter, 0.312 in. wall outer sheath surrounding a 2.125 in. outer-diameter rod filled with B<sub>4</sub>C powder. Lateral support for the absorber rods and center assembly was provided along their length by the intermediate support plates that have a small radial clearance to the shell as shown in Figure 5. Tie plates were alternated with the support plates to help limit deflection while minimizing flow blockage.

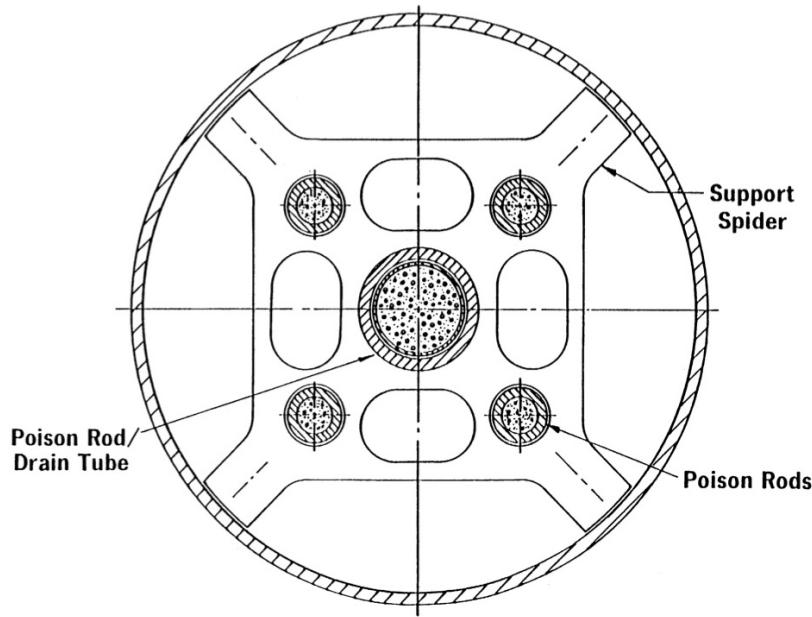


Figure 4. Knockout canister cross section at mid-plane.



Figure 5. Knockout canister ports and internals.

The influent flow was directed tangentially along the inner diameter of the shell, setting up a swirling action of the water within the canister. As the flow velocities decreased the larger particulate settled out and the water moved upwards, exiting the canister through a machined outlet in the head. A full flow screen (35 mesh) ensured that no large particles escaped from the canister.

The annulus between the 2.25 in. inner-diameter outer sheath and poison rod served as the drain tube for canister dewatering. The sheath was welded to the bottom support plate and has an outlet at the top welded to the upper head. The lower support plate has drain holes covered by a Rigimesh 20  $\mu\text{m}$  filter, which combined to form a drain sump in the lower head.

### 3.3 Filter Canister Description

As part of either the defueling water system or the fines/debris vacuum system, the filter canister was designed to remove very small debris particles from the water (see Figure 6). Externally, it was very similar to the other canister types, especially the knockout canister. The filter assembly module that fits inside the canister shell was designed by the Pall Trinity Micro Corporation and B&W to remove particulate in the range from 0.5 to 800 microns. Flow entered and exited the filter canister through 2-½ inch Hanson cam-and-groove quick disconnect fittings. After loading, the fittings were capped using special quick disconnect covers that use a Buna-N gasket good for at least 3 years of operation. These caps were replaced with the Thaxton plugs prior to shipment.

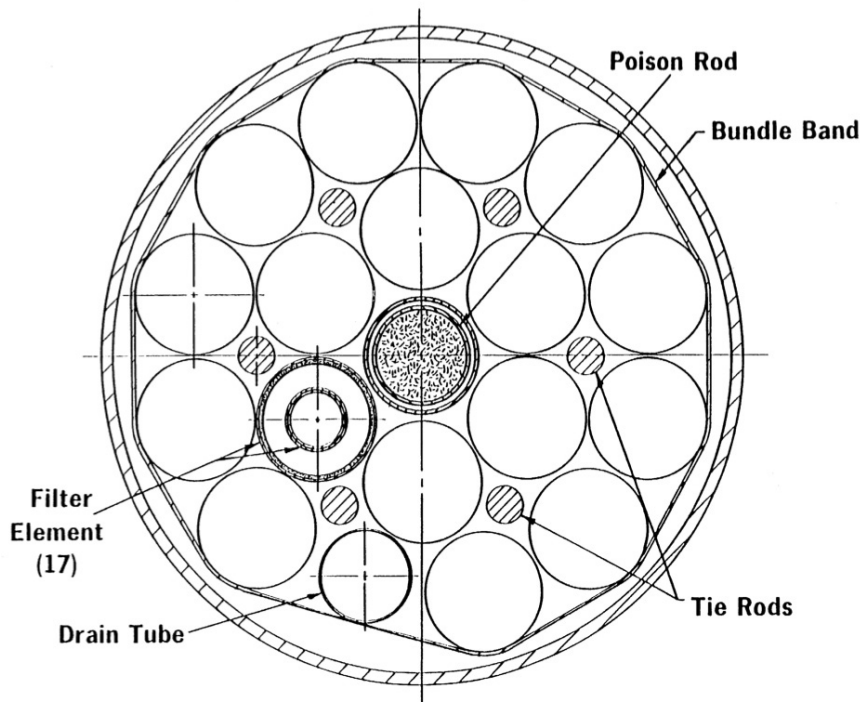


Figure 6. Filter canister cross section at mid-plane.

The internal filter assembly module consisted of a circular cluster of 17 filter elements, a drain line, and a neutron absorber assembly. Each filter element was made up of 11 filter modules joined axially, forming a continuous internal drain tube inside an annulus of filter media. The influent entered the upper plenum region, flowed down past the upper support plate, through the filter media, and down the element drain tube to the lower sump. The flow was from outside (shell side) to inside (internal drain tube side) with the filtered particulate remaining around the outer perimeter of the filter elements. The filtered water exited the canister via the drain line. The detailed design of the assembly started with the filter module followed by the longer filter element, and finally the assembly module itself.

The 11.0 in. long filter module shown in Figure 7 was the basic building block in the filter system. It was based on the concept of a pleated filter media forming an annulus around a central, perforated drain tube. Fabricated from a porous stainless steel material, the media was precoated with a sintered metal powder to control its pore size. The media and the center support tube were induction brazed to stainless steel end plates. Two bands were placed around the outer perimeter of each module. These bands restricted the unfolding of the pleats if a back-wash (reversed flow) was used to clean the particulate off the filter media.

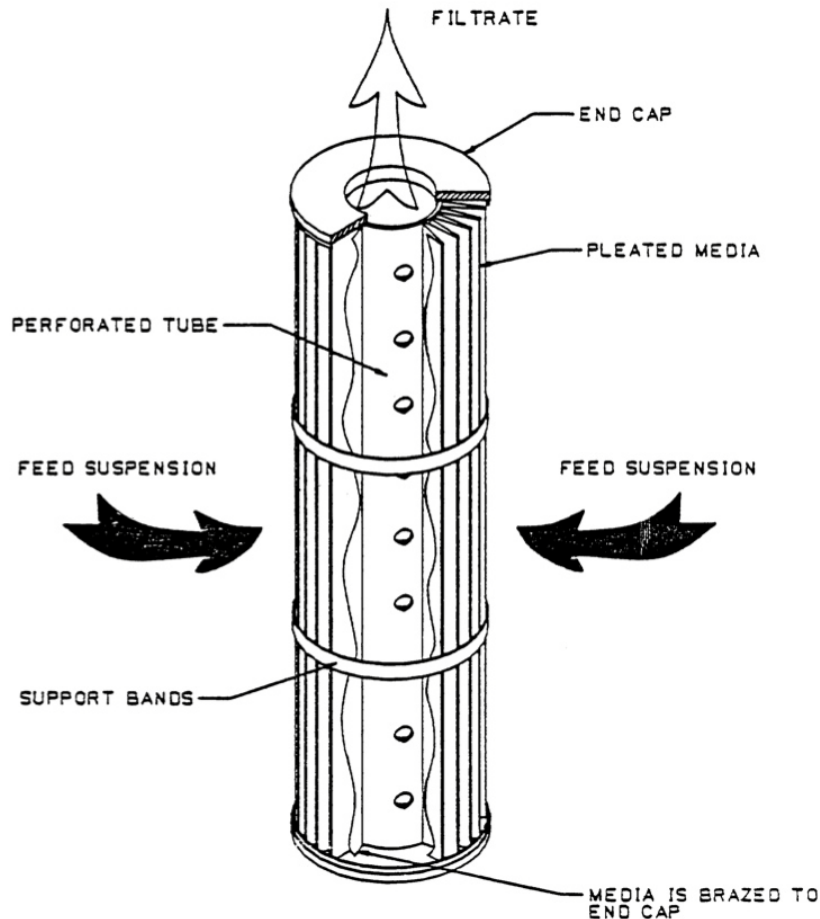


Figure 7. Filter module.

Eleven filter modules were stacked over a continuous 126 in. long one-eighth inch wall perforated tube and were then welded end-to-end to form a filter element. Only the ends of the module stack were welded to the continuous center drain tube. The drain tube was plugged at the top, forcing the water flow downward. This top plug mated with a hole in the upper support plate to restrain the lateral movement of the element. At its bottom end, the drain tube was seal-welded into a hole in the lower header.

The filter bundle assembly consisted of an array of 17 filter elements, a drain line, and an absorber assembly in a concentric circular pattern as shown in Figure 6 above. As previously described, the individual filter elements were held in place by the upper support plate and lower header. The lower header was welded to the outer shell of the canister to provide a boundary between the primary and secondary side of the filter system. The upper header was equipped with a series of openings to allow for the passage of the influent slurry into the filter section of the canister and to protect the filter media from direct impingement of particles carried in the influent flow. Six tie rods positioned the upper plate axially relative to the lower support plate. The upper plate was chocked into place with blocks that were tack welded to the outer shell.

### 3.4 TMI-2 Shipments

TMI-2 melted down in March of 1979. Extensive fuel damage occurred during this event, and some fission products were released. The water level was restored following this event. Defueling began in October of 1985. Therefore, this damaged fuel experienced water circulated cooling (in the reactor) for around 7 years; some leaching would have occurred during this time period. For shipment to Idaho



National Laboratory (INL), each canister was dewatered but they were not dried, so they still contained some water when shipped and received at INL. INL stored the canisters under water in the pool at Test Area North (TAN). The internal contents were flooded with demineralized water, which was added to the TMI water already in the canisters. Thus, some dissolved species in the water originated from the TMI water. The water inside the canister did not ever come in contact with the water in the storage pool.

Shipments from TMI to INL (and into wet storage) occurred from July 1986 to April 1990. Transfers to dry storage started in March of 1999 and ended in April 2001. Therefore the TMI-2 canisters were in wet storage for a minimum of about 9 years and a maximum of about 15 years.

When each fuel canister was loaded with fuel debris at TMI, a sketch was made of the canister with general notes on what was loaded into each fuel canister. Three of these sketches are pictured in Figures 8, 9, and 10.

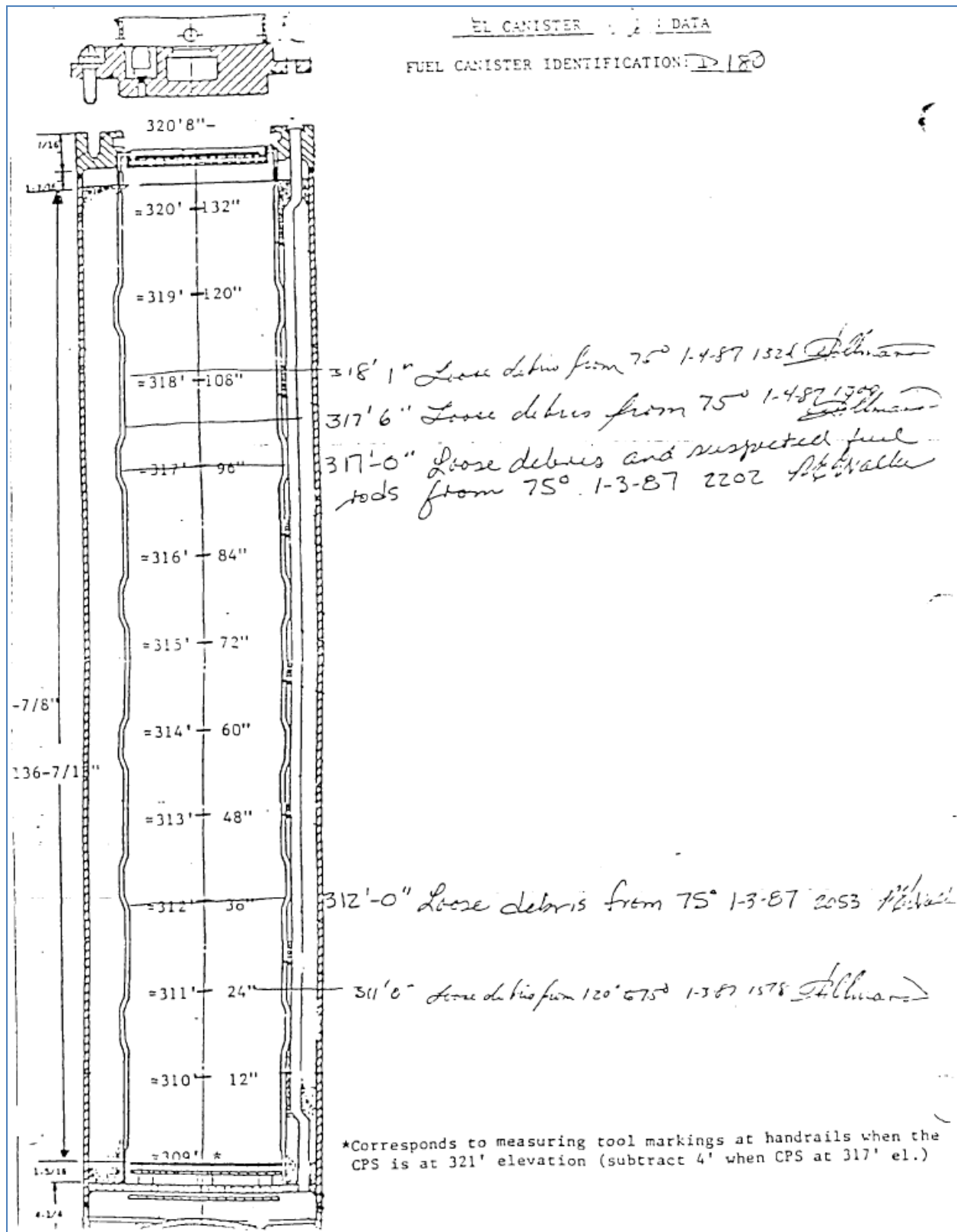


Figure 8. Canister loading data for Canister D-180.

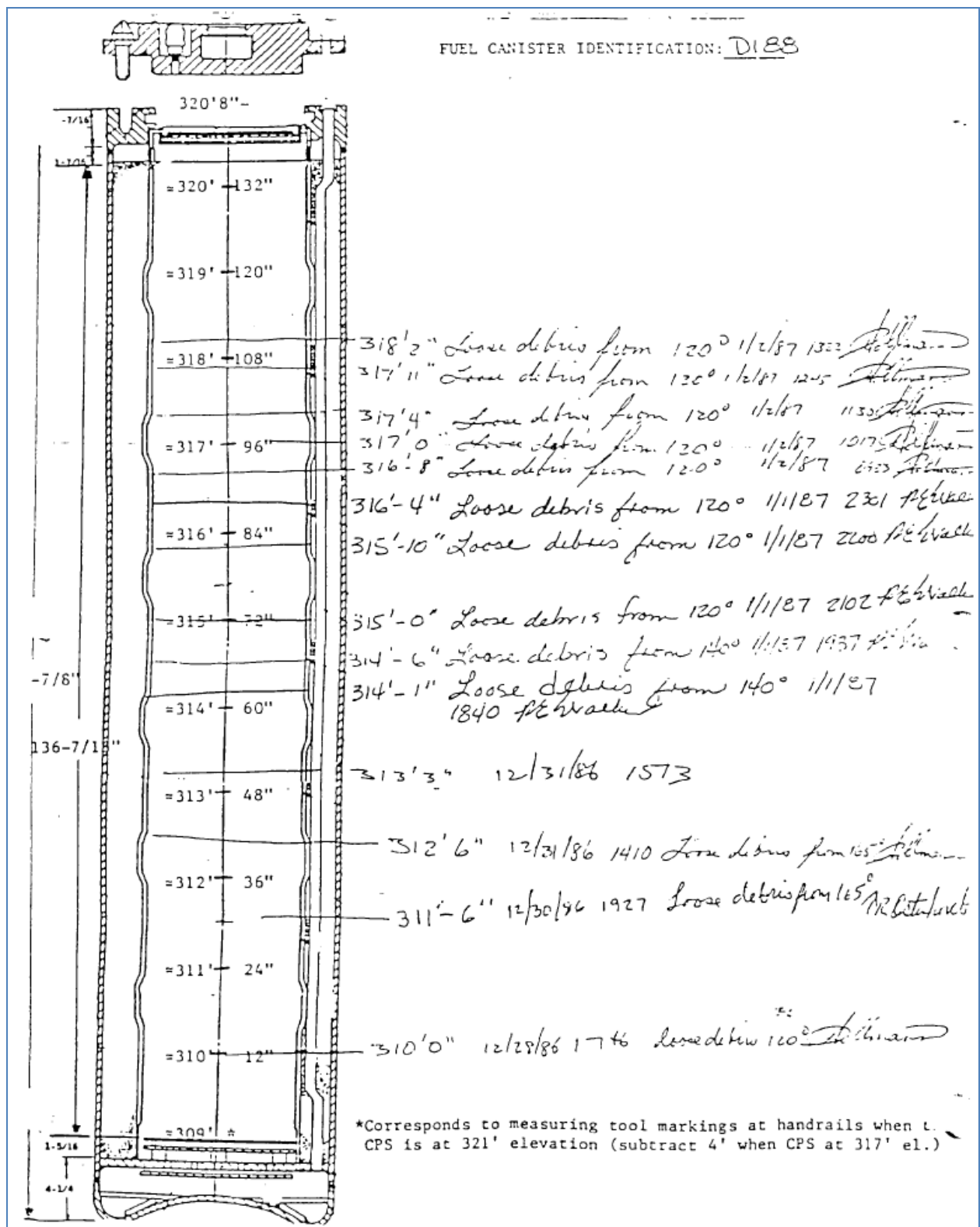


Figure 9. Canister loading data for Canister D-188.

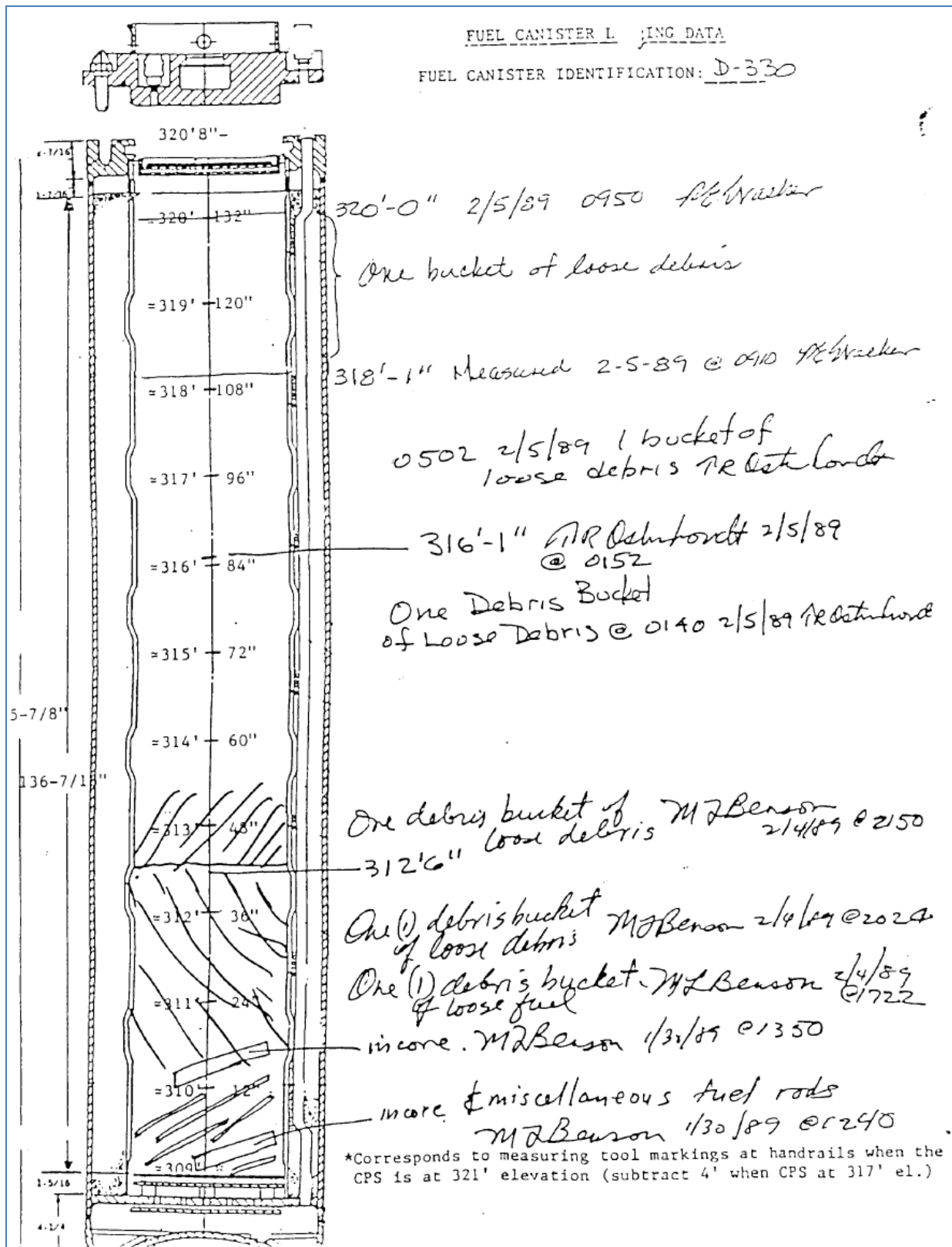


Figure 10. Canister loading data for Canister D-330.

### 3.5 Leaching Data

In December 1995, water in five of the canisters was analyzed for elements and radionuclides that had leached into the water during wet storage. The water sample data for canisters D-180, D-188, D-330, F-462, and K-506 (i.e., three fuel debris canisters, one filter canister, and one knockout canister) are shown in Tables 1 and 2. Canisters D-180 and D-188 were in wet storage for about 8 years when sampled and the other three canisters were in wet storage about 6 years when sampled. The maximum and minimum amounts are shown for each element or isotope given the uncertainty of the sampling/analytical method. The less than (<) symbol indicates the result was below detection limits. Appendix A includes a discussion of the sampling/analytical methods used to determine concentrations of elements and radionuclides.

The pH of each canister was measured at 8.0 using a pH paper test (except for canister D-330, which had a pH of 8.5). Table 3 provides the radioactivity of the canister water for each canister.

In order to better visualize the data, the data in Tables 1 and 2 are plotted in Figures 11–15. Also, Figure 16 shows the maximum and minimum sample results for the isotopes for each of the canisters.

Table 4 provides additional pertinent data for each of the five canisters that were sampled.

Table 1. Sample results for materials in canister water.

Minimum Detectable Limit (MDL)	Canister D-180		Canister D-188		Canister D-330		Canister F-462		Canister K-506		Sampling/Analytical Method
	Max (mg/L)	Min (mg/L)	Max (mg/L)	Min (mg/L)	Max (mg/L)	Min (mg/L)	Max (mg/L)	Min (mg/L)			
Arsenic (As)	0.2 mg/L	< 2.00E-01	0.00E+00	< 2.00E-01	0.00E+00	< 2.00E-01	0.00E+00	< 2.00E-01	0.00E+00	Inductively coupled plasma mass spectrometry (ICP-MS)	
Barium (Ba)	0.005 mg/L	2.05E-02	2.05E-02	5.40E-02	5.40E-02	9.65E-02	9.65E-02	8.50E-02	8.50E-02	Inductively coupled plasma mass spectrometry (ICP-MS)	
Boron (B)	3 mg/L	9.76E+02	9.76E+02	7.83E+02	7.83E+02	7.39E+02	7.39E+02	8.62E+02	8.62E+02	Inductively coupled plasma mass spectrometry (ICP-MS)	
Cadmium (Cd)	0.01 mg/L	2.05E-02	2.05E-02	2.00E-02	2.00E-02	3.35E-02	3.35E-02	5.75E-02	5.75E-02	Inductively coupled plasma mass spectrometry (ICP-MS)	
Calcium (Ca)	0.025 mg/L	1.69E-01	1.69E-01	1.63E-01	1.63E-01	1.55E+01	1.55E+01	4.99E-01	4.99E-01	Inductively coupled plasma mass spectrometry (ICP-MS)	
Chromium (Cr)	0.005 mg/L	< 5.00E-03	0.00E+00	< 5.00E-03	0.00E+00	< 5.00E-03	0.00E+00	1.05E-02	1.05E-02	Inductively coupled plasma mass spectrometry (ICP-MS)	
Lead (Pb)	0.1 mg/L	< 1.00E-01	0.00E+00	< 1.00E-01	0.00E+00	< 1.00E-01	0.00E+00	< 1.00E-01	0.00E+00	Inductively coupled plasma mass spectrometry (ICP-MS)	
Lithium (Li)	0.05 mg/L	6.00E-02	6.00E-02	7.50E-02	7.50E-02	< 5.00E-02	0.00E+00	< 5.00E-02	0.00E+00	[not known]	
Magnesium (Mg)	0.1 mg/L	< 1.00E-01	0.00E+00	< 1.00E-01	0.00E+00	5.40E+00	5.40E+00	< 1.00E-01	0.00E+00	Inductively coupled plasma mass spectrometry (ICP-MS)	
Mercury (Hg)	0.11 mg/L	< 1.1E-01	0.00E+00	< 1.1E-01	0.00E+00	< 1.1E-01	0.00E+00	< 1.1E-01	0.00E+00	[not known]	
Selenium (Se)	0.2 mg/L	< 2.00E-01	0.00E+00	< 2.00E-01	0.00E+00	< 2.00E-01	0.00E+00	< 2.00E-01	0.00E+00	Inductively coupled plasma mass spectrometry (ICP-MS)	
Silicon (Si)	0.15 mg/L	6.57E-01	6.57E-01	6.05E-01	6.05E-01	1.99E+00	1.99E+00	3.45E+00	3.45E+00	Inductively coupled plasma mass spectrometry (ICP-MS)	
Silver (Ag)	0.02 mg/L	< 2.00E-02	0.00E+00	< 2.00E-02	0.00E+00	< 2.00E-02	0.00E+00	3.65E-02	3.65E-02	Inductively coupled plasma mass spectrometry (ICP-MS)	
Sodium (Na)		2.86E+02	2.86E+02	2.46E+02	2.46E+02	3.31E+02	3.31E+02	2.66E+02	2.66E+02	Inductively coupled plasma mass spectrometry (ICP-MS)	
Nitrate (NO <sub>3</sub> <sup>-</sup> )	0.821 mg/L	< 8.21E-01	0.00E+00	< 8.21E-01	0.00E+00	< 8.21E-01	0.00E+00	< 8.21E-01	0.00E+00	Ion Chromatography	
Chloride (Cl <sup>-</sup> )	0.181 mg/L	1.64E+00	1.39E+00	3.31E+00	3.06E+00	7.42E+00	7.18E+00	4.91E+00	4.66E+00	Ion Chromatography	
Bromide (Br <sup>-</sup> )	0.09 mg/L	2.64E-01	2.64E-01	< 9.00E-02	0.00E+00	< 9.00E-02	0.00E+00	2.23E-01	2.23E-01	Ion Chromatography	
Uranium (U)	0.006 mg/L	< 6.00E-03	0.00E+00	< 6.00E-03	0.00E+00	< 6.00E-03	0.00E+00	< 6.00E-03	0.00E+00	Extraction Fluorophotometric Determination	

Table 2. Sample results for radionuclides in canister water (as of December 1995).

	Canister D-180		Canister D-188		Canister D-330		Canister F-462		Canister K-506		Sampling/Analytical Method
	Max (mg/L)	Min (mg/L)	Max (mg/L)	Min (mg/L)	Max (mg/L)	Min (mg/L)	Max (mg/L)	Min (mg/L)	Max (mg/L)	Min (mg/L)	
<b>Pu238</b>	4.92E-06	0.00E+00	< 4.53E-08	0.00E+00	2.75E-06	0.00E+00	4.67E-06	2.71E-06	< 1.74E-07	0.00E+00	Ion Chromatography separation & detection by alpha spectrometry Ion Chromatography separation & detection by alpha spectrometry Ion Chromatography separation & detection by alpha spectrometry Ion Chromatography separation & detection by alpha spectrometry Ion Chromatography separation & detection by alpha spectrometry Ion Chromatography separation & detection by alpha spectrometry Ion Chromatography separation & detection by alpha spectrometry Ion Chromatography separation & detection by alpha spectrometry Ion Chromatography separation & detection by alpha spectrometry Ion Chromatography separation & detection by alpha spectrometry
<b>Pu239</b>	6.10E-04	0.00E+00	1.18E-03	0.00E+00	3.57E-04	0.00E+00	7.67E-05	0.00E+00	9.41E-04	4.62E-04	
<b>Np237</b>	1.02E-01	5.99E-02	1.79E-03	0.00E+00	2.07E-01	1.47E-01	1.90E-03	0.00E+00	1.88E-02	0.00E+00	
<b>Am241</b>	3.40E-06	0.00E+00	1.26E-05	0.00E+00	1.22E-05	0.00E+00	9.65E-06	4.16E-06	5.73E-06	0.00E+00	
<b>Th228</b>	1.11E-09	0.00E+00	2.53E-08	0.00E+00	2.06E-08	0.00E+00	2.27E-08	0.00E+00	< 5.11E-09	0.00E+00	
<b>Th230</b>	3.93E-04	0.00E+00	9.85E-04	0.00E+00	< 1.27E-04	0.00E+00	8.23E-04	0.00E+00	7.46E-04	0.00E+00	
<b>Th232</b>	1.14E+02	0.00E+00	< 2.22E+00	0.00E+00	< 2.22E+00	0.00E+00	< 2.21E+00	0.00E+00	1.05E+02	0.00E+00	
<b>Tc99</b>	6.48E-03	2.86E-03	5.94E-02	5.50E-02	1.93E-02	1.54E-02	3.49E-03	0.00E+00	4.27E-02	3.86E-02	
<b>Sr90</b>	7.60E-03	7.60E-03	3.79E+03	3.79E+03	9.08E+02	9.08E+02	2.14E+03	2.14E+03	2.00E+03	2.00E+03	
<b>H3 (Tritium)</b>	1.09E-06	1.09E-06	1.58E-06	1.58E-06	9.52E-07	9.52E-07	1.26E-06	1.26E-06	1.11E-06	1.11E-06	
<b>Cs134</b>	4.22E-06	3.56E-06	5.37E-06	4.57E-06	1.73E-06	1.52E-06	No Data	No Data	3.80E-06	3.31E-06	Gamma Spectroscopy
<b>Cs137</b>	3.60E-02	3.30E-02	4.47E-02	4.11E-02	1.41E-02	1.29E-02	9.90E-04	9.16E-04	2.90E-02	2.66E-02	Gamma Spectroscopy

Table 3. Canister water radioactivity (as of December 1995).

Canister	Gross Alpha Beta Radioactivity	
D-180	5.72E+06 (± 4.5E+04) pCi/mL	2.12E+08 (± 1.7E+06) Bq/L
D-188	5.74E+06 (± 4.5E+04) pCi/mL	2.12E+08 (± 1.7E+06) Bq/L
D-330	1.68E+06 (± 2.5E+04) pCi/mL	6.23E+07 (± 9.3E+05) Bq/L
F-462	6.42E+05 (± 1.6E+04) pCi/mL	2.38E+07 (± 5.9E+05) Bq/L
K-506	3.70E+06 (± 3.6E+04) pCi/mL	1.37E+08 (± 1.3E+06) Bq/L

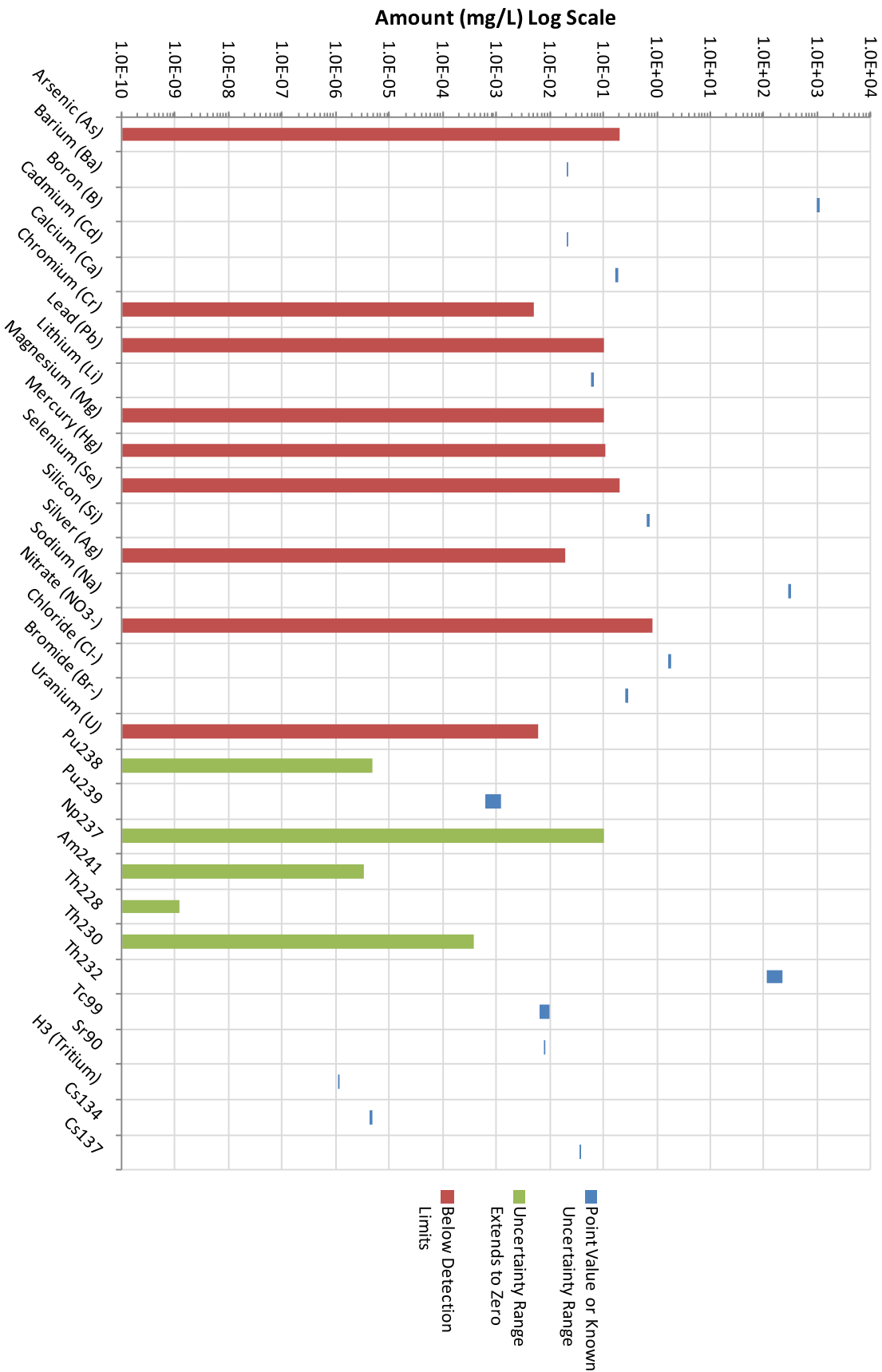


Figure 11. Sample results plot for Canister D-180.



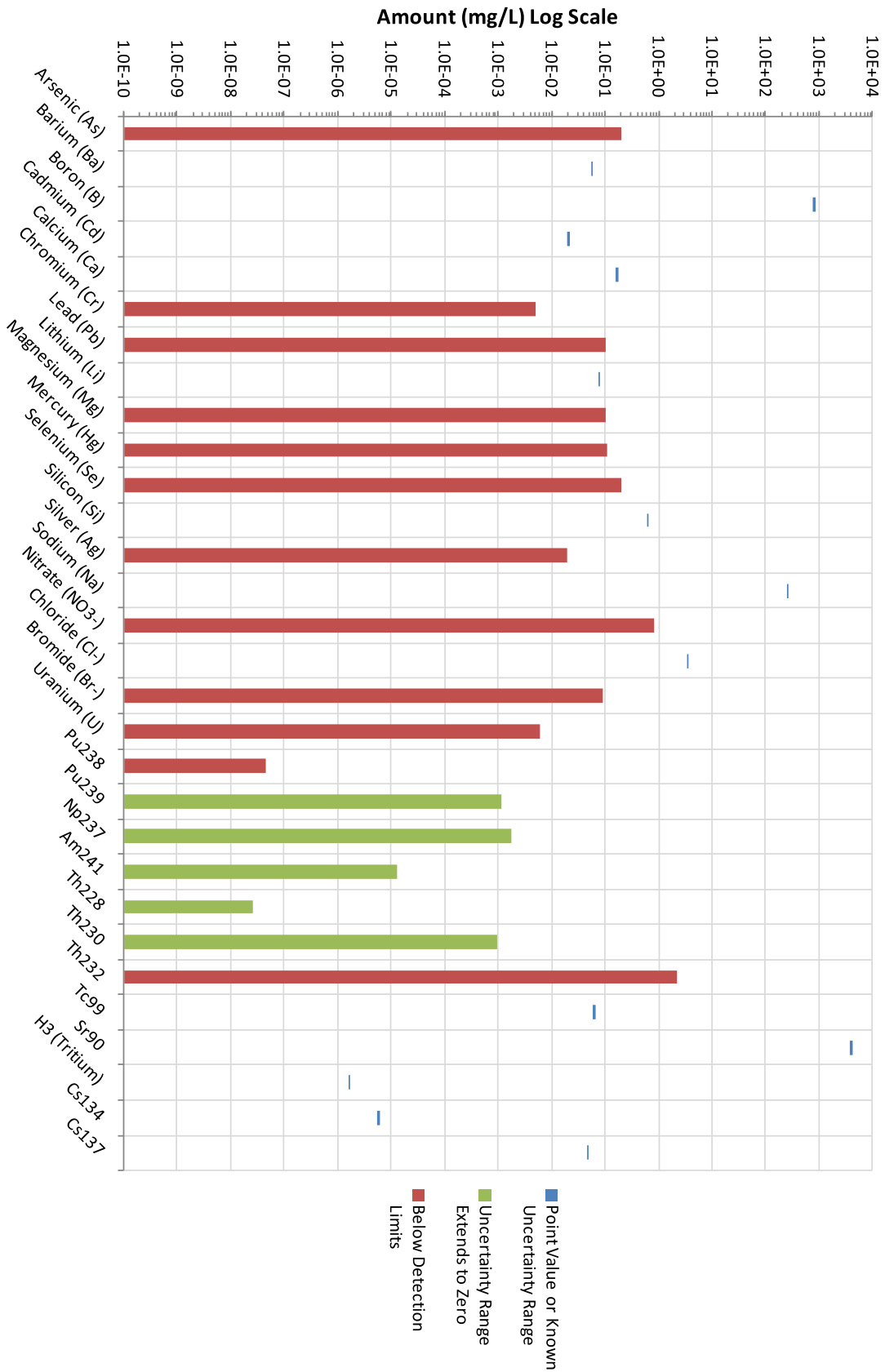
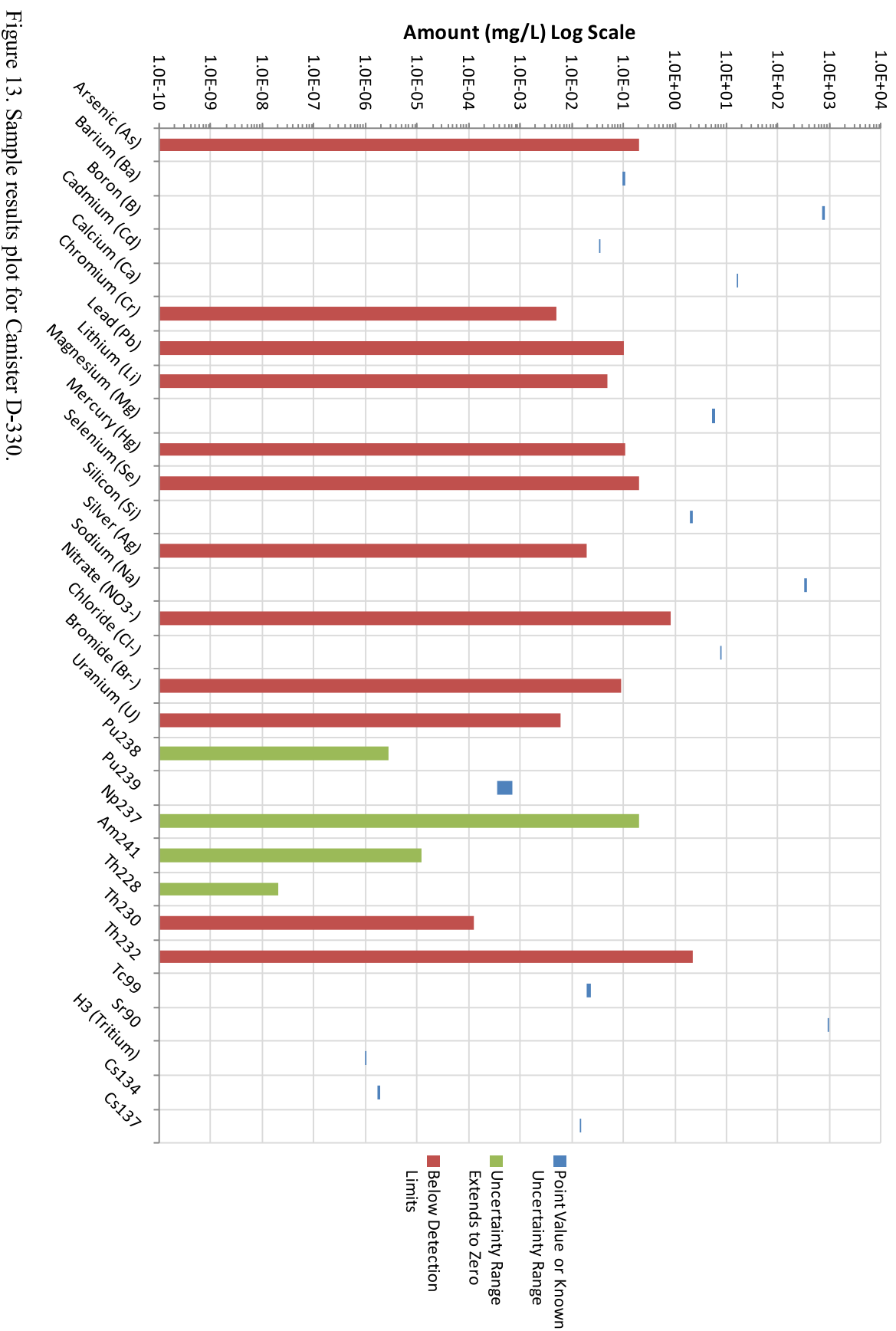


Figure 12. Sample results plot for Canister D-188.



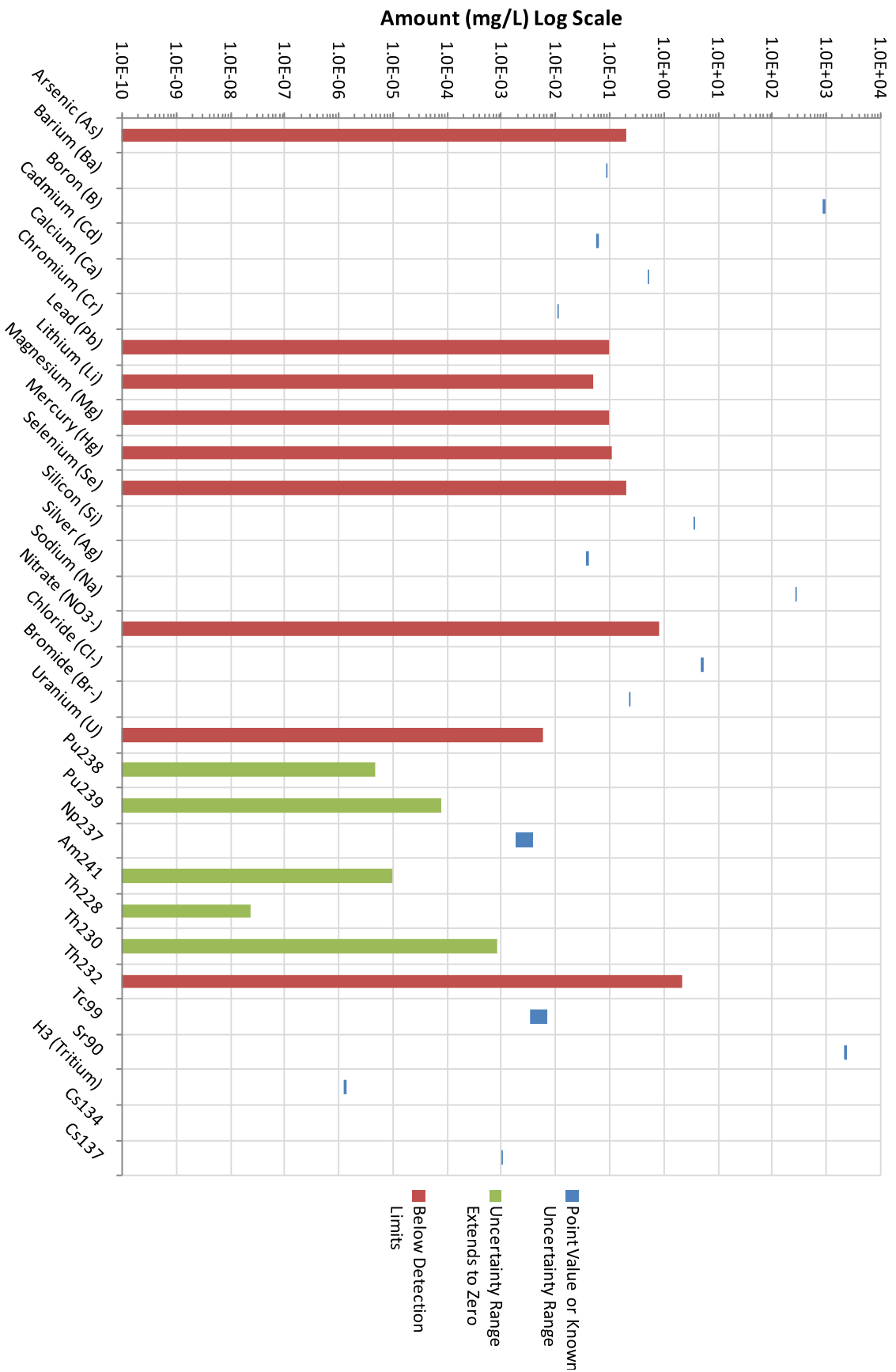


Figure 14. Sample results plot for Canister F-462.

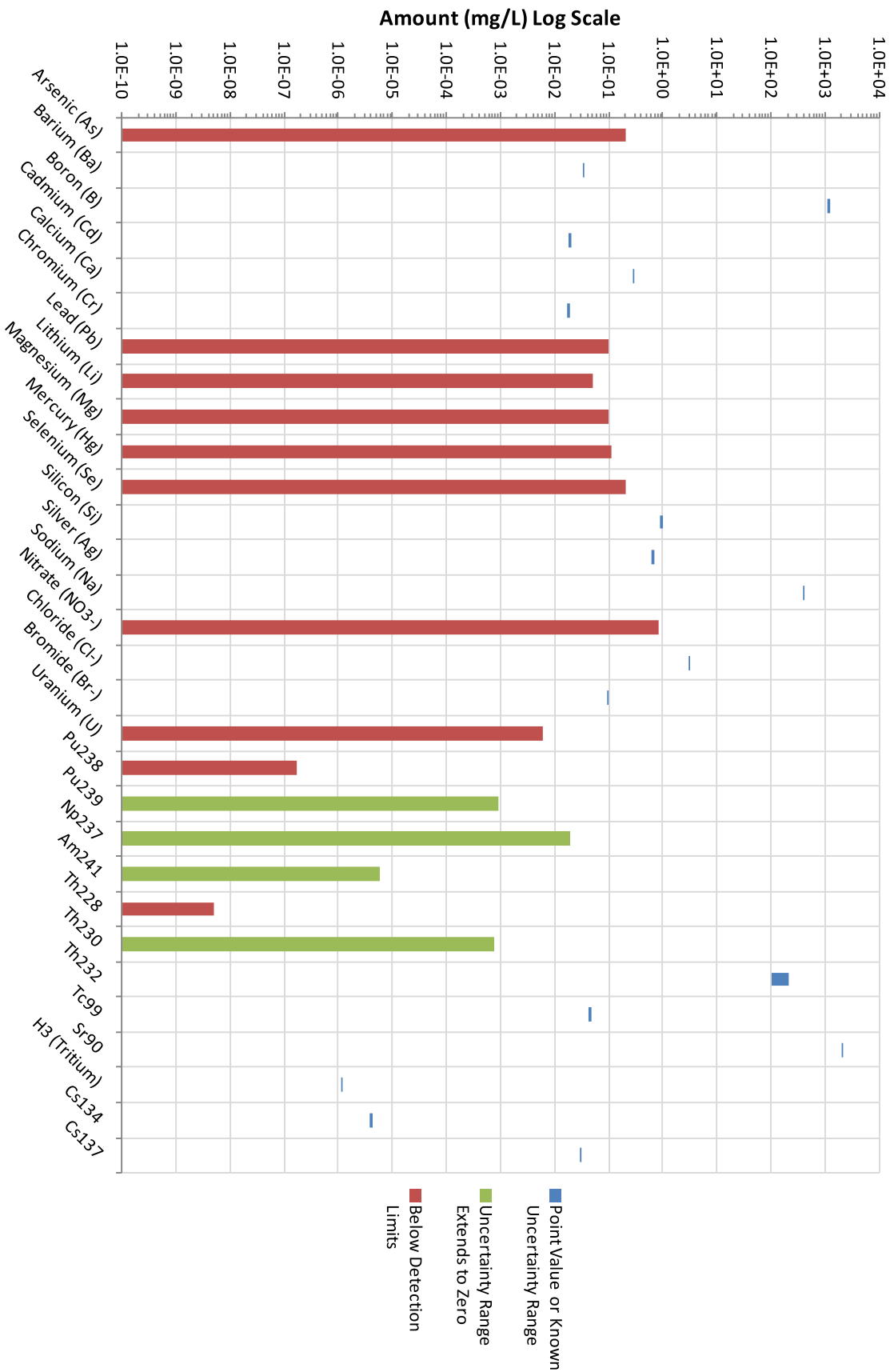


Figure 15. Sample results plot for Canister K-506.

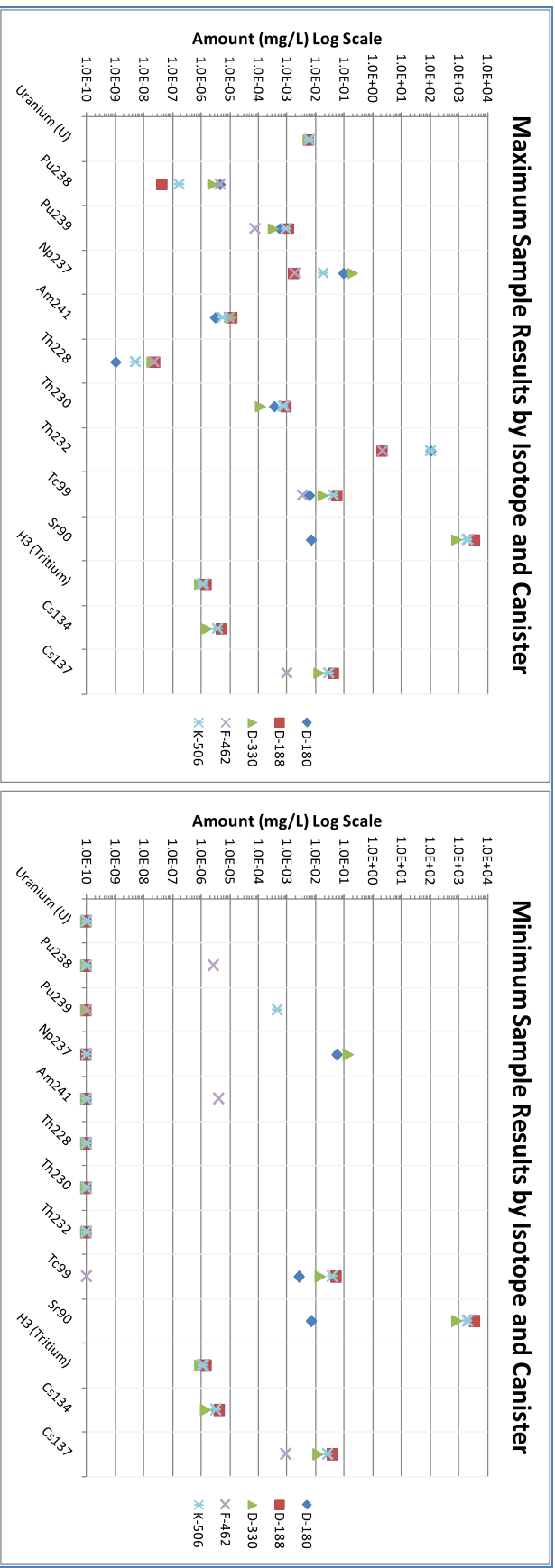


Figure 16. Maximum and minimum results plot.

Table 4. Canister data (for shipments to INL).

Canister ID	Canister Weight (kg)						Debris			Void		Estimated Total U (g)	Estimated Total Pu (g)
	Empty	Full	De-watered	Core Debris	Non Debris	Water Remaining	Total Payload	Density (kg/L)	Volume (L)				
D-180	542	1,393	1,315	743	0	29	772	7	72		394,100 (± 41,800)	802 (± 56)	
D-188	542	1,405	1,317	746	0	29	775	7	81		395,300 (± 41,900)	805 (± 84)	
D-330	538	1,406	1,327	767	0	22	789	7	78		402,700 (± 42,700)	820 (± 86)	
F-462	662	1,218	1,101	310	18	111	439	3	120		162,500 (± 36,700)	331 (± 75)	
K-506	458	1,471	1,324	842	0	23	865	5	146		441,900 (± 99,900)	900 (± 203)	

### 3.6 Uranium and Plutonium Estimates

This section provides a brief explanation of how the amount of uranium and plutonium were estimated for each canister (as shown in Table 4). First, ORIGEN code was used to model the final amounts of material left in the core based on the burnup and core geometry; this provided a total amount of uranium and plutonium. Next, using the canister loading data, the contents were divided into three classes:

1. Recognized fuel assemblies, which were known lengths of more or less intact fuel assemblies; most of these were identifiable so that their initial enrichment (2.96, 2.64, or 1.98%) was known.
2. Structural material, which was any piece of material for which the weight could be estimated and which contained no special nuclear material, except perhaps as surface contamination.
3. Debris, which was any other core material in the canister, including parts of fuel pins, parts of structural material, pieces of resolidified molten material, chips from drilling or cutting operations, and other material.

Using the loading data, the amount of uranium and plutonium was estimated for each canister. Once all canisters were estimated, the estimated amounts were scaled slightly so that they agreed with the total estimated uranium and plutonium. Because these were purely estimates, the uncertainty is quite high as seen in Table 4.

### 3.7 Discussion of Leachability

Based on the results of the sampling of canister water, the major dissolved components were: boron, sodium, strontium, and thorium (in two of the five canisters). The boron very likely originated from the borated water that was in the reactor coolant water and canisters at TMI-2 and the boric acid residue deposits on the fuel that would have dissolved upon addition of water at TAN.

The sodium (although still at relatively low levels at about 250 mg/L) also came from the leftover reactor coolant water at TMI-2 following the accidental meltdown. This coolant water had NaOH added to it to maintain the pH level above 7.5. Some of this water from TMI-2 remained in the canisters, since the canisters were not completely dried before shipment.

The amount of strontium in the water sample agrees fairly well with the leach rates published in Reference 3 (International Atomic Energy Agency [IAEA]; leach test results given in Section 4.1 of Reference 3. The sample results for Sr-90 from canister D-188 in Table 2 ( $3.79 \times 10^3$  mg/L) multiplied by the amount of water in the canister (100 L) gives 379 g of strontium. Using  $220 \text{ m}^2/\text{m}^3$  as an estimate<sup>9</sup> of surface area per volume for spent fuel rubble and calculating  $0.14468 \text{ m}^3$  for the volume of fuel rubble in Canister D-188 yields  $3.18 \times 10^5 \text{ cm}^2$  as an estimate of fuel debris surface area. Then taking 379 g divided by  $3.18 \times 10^5 \text{ cm}^2$  and dividing by 8 years yields an estimate of  $4 \times 10^{-7} \text{ g/cm}^2/\text{day}$  for Sr-90. The IAEA leach test result for Sr-90 + Y-90 in Table 6 was  $3.3 \times 10^{-6} \text{ g/cm}^2/\text{day}$  (for the NaCl solution). It is expected that the estimated TMI leach rate would be lower because this estimate does not include the strontium that leached out during the 8 years of storage in the reactor core at TMI. The IAEA leach rate tests only went out to 1.3 years (and tend to decline over time). Also, the IAEA test result includes Y-90 and the TMI estimate does not.

Using the same logic as explained in the previous paragraph, the leach rate can be calculated for the other species in Table 2. The average result (of the maximum concentration) for all five canisters is shown in Table 5. Note that these leach rates are all very low if not negligible in magnitude. With a uranium concentration at less than  $6 \times 10^{-3} \text{ mg/L}$  in the sample water, this results in a calculated leach rate for uranium of  $< 6 \times 10^{-13} \text{ g/cm}^2/\text{day}$ .

Table 5. Calculated average (of the maximum) leach rates for all five canister sample results.

	Average (g/cm <sup>2</sup> /day)
Pu238	3E-16
Pu239	8E-14
Np237	9E-12
Am241	1E-15
Th228	2E-18
Th230	8E-14
Th232*	< 3E-10
Tc99	3E-12
H3 (Tritium)	2E-16
Cs134	5E-16
Cs137	3E-12

\* Excluding canister D-180 and K-506 for Th-232.

The higher amounts of Th-232 that showed up in the sample results for Canisters D-180 and K-506 may most likely be the result of a sampling error or contamination. The sample result of Th-232 for the other three canisters was below the detection limit. Using an estimate from ORIGEN data for TMI fuel debris, it is estimated that the total amount of Th-232 that would be in a canister of TMI debris would be about 2 mg. However, the sample results for canister D-180 shows about 114 mg/L dissolved in the water, which would be very unlikely. The solubility of thorium oxide in water is very low, which also contributes to the assumption that the Th-232 sample results for Canisters D-180 and K-506 are outliers.

### 3.8 Corrosivity of Solutions

The solutions all had a pH of 8.0, except for Canister D-330, which had a pH of 8.5. The chloride concentrations are extremely low, ranging from  $4.26 \times 10^{-5}$  to  $2.06 \times 10^{-4}$  M (1.51 to 7.30 ppm<sub>w</sub>). The source was likely the demineralized water that was added to the canisters. Typical chloride concentrations in demineralized water range from  $8.5 \times 10^{-5}$  to  $3.4 \times 10^{-4}$  M (3 to 12 ppm<sub>w</sub>). The overall system was nonoxidizing. The conditions are generally noncorrosive toward stainless steel. The canisters had been in contact with the water for at least 6 years.

## 4. LOSS OF FLUID TEST FACILITY (LOFT) DATA

The Loss of Fluid Test (LOFT) facility at INL was a scale model of a large pressurized water reactor (LPWR). The intent of the facility was to model the nuclear, thermal-hydraulic phenomena that would take place in an LPWR during a loss-of-coolant accident (LOCA) sequence. The general philosophy in scaling coolant volumes and flow areas in LOFT was to use the ratio of the LOFT core [50 MW(t)] to a typical LPWR core [3,000 MW(t)]. In general, components used in LOFT were similar in design to those of an LPWR. Because of scaling and component design, the LOFT LOCA closely modeled an LPWR LOCA.

On July 9, 1985, the LP-FP-2 experiment was conducted at the LOFT facility. Its principal objectives were to determine the fission product release from the fuel during a severe fuel damage scenario and the subsequent transport of these fission products in a predominantly vapor/aerosol environment. This was the largest severe fuel damage experiment ever conducted, and serves as an important benchmark between smaller-scale tests and the TMI-2 accident.<sup>5</sup>

The results from the LP-FP-2 experiment were captured in a series of reports: *Postirradiation Examination Data and Analyses for OECD LOFT Fission Product Experiment LP-FP-2, Volumes 1 & 2*, *OECD LOFT Fission Product Experiment LP FP-2 Data Report*, *Containment Analysis Report for LOFT Experiment LP FP-2*, and *Experiment Analysis and Summary Report for OECD LOFT Project Fission Product Experiment LP-FP-2*.<sup>5,6,7,8</sup>

The *Postirradiation Examination Data and Analyses for OECD LOFT Fission Product Experiment LP-FP-2* report presents data and analysis from the postirradiation examinations of the LP-FP-2 fuel bundle. Several images of the postirradiation nondestructive and destructive examinations are included in the report. Also, information is presented on the material behavior and interactions that occurred within the fuel bundle during this severe core damage experiment.<sup>5</sup>

The *OECD LOFT Fission Product Experiment LP FP-2 Data Report* presents the initial conditions, sequence of events, thermal-hydraulic data, gamma spectrometer data, grab-sample data, and the postirradiation examination data of the filters and coupon devices that were obtained for the LP-FP-2 experiment. Several results, presented in the form of tables and charts, are included in this report.<sup>6</sup>

The *Containment Analysis Report for LOFT Experiment LP FP-2* report presented the findings for fission product transport and deposition within the LOFT containment vessel. Leaks from the blowdown suppression tank and the primary coolant system allowed small quantities of noble gases and iodine to be released to the containment vessel. The purpose of this report was to determine the release fractions of the noble gases, iodine, and cesium to the containment vessel and to determine the primary source of this material (e.g., blowdown suppression tank or primary coolant system).<sup>7</sup>

The *Experiment Analysis and Summary Report for OECD LOFT Project Fission Product Experiment LP-FP-2* report presents the best estimate post-test calculation of the thermal-hydraulic and fission product transport analysis of the LP-FP-2 experiment. Sensitivity calculations were also presented where key phenomena were known to influence the results. The analysis presented in this report includes the combined efforts of several computer codes, including SCDAP/RELAP5, FASTGRASS, CORSOR, SOLGASMIX-PV, TRAP-MELT2, PULSE, and interpretation of the analysis results and comparisons with the measured data.<sup>8</sup>

## 4.1 Leaching Data

Information about leaching is discussed in the following documents:

- *OECD LOFT Fission Product Experiment LP FP-2 Data Report*, Section 4.<sup>6</sup>
- *Experiment Analysis and Summary Report for OECD LOFT Project Fission Product Experiment LP-FP-2*, Section 4.<sup>8</sup>

The references listed above contain a large amount of detailed information about fission product release during and immediately following a loss of fluid event in a reactor. Some summary results are shown in Tables 6 and 7. Table 6 comes from Section 5.3 of Reference 6, and Table 7 comes from Section 5.4 of Reference 6. The results in Table 7 assume that the cesium and iodine concentrations were uniformly distributed throughout the primary coolant system with no contribution for plateout. Because of these assumptions, the results (in Table 7) represent a lower bound for the release fractions.



Table 6. Cumulative release fractions of the damaged fuel to the blowdown suppression tank (BST).

Isotope	Calculated Fuel Inventory (Ci)	Liquid (Ci)	Gas (Ci)	Total (Ci)	Cumulative Release Fractions to the BST
I-131	47570.0	29.96	0.0065	29.97	0.063%
Cs-136	100.2	0.287	-	0.287	0.29%
Cs-137	144.6	0.361	-	0.361	0.25%
Kr-85	17.3	-	0.310	0.310	1.79%
Xe-131m	237.2	-	3.88	3.88	1.64%
Xe-133	110400.0	-	1939.0	1939.0	1.76%
Xe-133m	3262.0	-	47.9	47.9	1.47%
Te-132	90890.0	8.37	-	8.37	0.0092%
Ba-140	80250.0	21.82	-	21.82	0.027%
Ru-103	18110.1	0.0213	-	0.0213	0.00012%

Table 7. Estimated fission product retention in the primary coolant system.

Isotope	Calculated Fuel Inventory (Ci)	Liquid Inventory (Ci)	Release Fraction
I-131	$4.757 \times 10^4$	$6.57 \times 10^3$	13.8%
I-132	$8.939 \times 10^4$	$1.71 \times 10^4$	19.1%
I-133	$2.147 \times 10^5$	$2.80 \times 10^4$	13.0%
I-134	$3.011 \times 10^5$	$5.21 \times 10^4$	17.3%
Cs-137	$1.446 \times 10^2$	$2.69 \times 10^1$	18.6%

## 4.2 Metallography

Information about metallography is discussed in the following document:

- *Postirradiation Examination Data and Analyses for OECD LOFT Fission Product Experiment LP-FP-2*, Sections 3 and 4.<sup>5</sup>

## 5. OTHER DATA

A search of past literature for information on leaching of spent fuel turned up several references. Y. B. Katayama produced reports (1976,<sup>1</sup> 1979,<sup>2</sup> and 1980<sup>3</sup>) on leaching of spent fuel. The *Status Report on LWR Spent Fuel IAEA Leach Tests* (1980<sup>3</sup>) appears to be best source of information and data. In this report, spent LWR (unclad) fuel with a burnup of 28,000 MWd/MTU was leach-tested at 25°C. Leach rates were determined from tests conducted in five different solutions: deionized water, sodium chloride solution, sodium bicarbonate solution, calcium chloride solution, and a brine solution.

## 5.1 IAEA Leach Test Results

The *Status Report on LWR Spent Fuel IAEA Leach Tests*<sup>3</sup> provides the leach rates for Sr-90 + Y-90, Ru-106, Cs-137, Ce-144, Eu-154, Pu-239 + Pu-240, Cm-244, and total uranium in five different solutions for 467 days. The results are presented in Table 8 for the end of the experiment at 467 days for the five different solutions.

Table 8. IAEA leach rates for 28,000 MWd/MTU spent fuel at 25°C at 467 days (g/cm<sup>2</sup>-day).

Isotope	Saturated Brine	CaCl <sub>2</sub> Solution	NaCl Solution	NaHCO <sub>3</sub> Solution	Deionized Water
Cm-244	3.1E-6	9.1E-8	4.0E-6	1.5E-7	1.5E-5
U	6E-7	3E-8	2E-6	1E-6	4E-6
Sb-125	3.8E-6	7.6E-8	3.5E-6	7.0E-6	1.3E-5
Ce-144	9.4E-7	1.1E-7	3.5E-6	1.0E-7	1.2E-5
Sr-90 + Y-90	3.1E-6	1.4E-7	3.3E-6	8.2E-7	9.6E-6
Cs-137	3.8E-6	8.9E-7	6.1E-6	3.3E-6	1.2E-5
Eu-154	2.2E-6	1.2E-7	6.9E-6	9.9E-6	1.5E-5
Pu-239 + Pu-240	3.7E-6	1.6E-7	3.0E-6	2.1E-7	1.1E-5
Ru-106	3.8E-7	3.7E-7	5.1E-7	1.3E-7	1.8E-6

Of the five solutions studied, deionized water produced the highest average elemental leach rate. The leach rates in the bicarbonate solution were second lowest, with the CaCl<sub>2</sub> solution exhibiting the lowest leach rates. The two brines were intermediate. Cesium had a high leach rate in two solutions (saturated brine and CaCl<sub>2</sub>). Europium had the highest leach rate in deionized water and in NaHCO<sub>3</sub>. Ruthenium had the lowest leach rate in three solutions (deionized water, NaCl and saturated brine). Cerium had the lowest elemental leach rate in NaHCO<sub>3</sub> and uranium the lowest in CaCl<sub>2</sub> solution.

## 5.2 Leaching of Irradiated LWR Fuel in a Simulated Post-Accident Environment

Another excellent source of leaching data is the ORNL report, *Leaching of Irradiated Light-Water-Reactor Fuel in a Simulated Post-Accident Environment*.<sup>4</sup> In this report, experiments were designed to investigate leaching in a reactor vessel environment using a borate solution as the leachant.

## 6. REFERENCES

1. Y. B. Katayama, *Leaching of Irradiated LWR Fuel Pellets in Deionized and Typical Groundwater*, BNWL-2057, Pacific Northwest Laboratories, Richland, WA, 1976.
2. Y. B. Katayama, *Spent Fuel Leach Test*, PNL-2982, Battelle Pacific Northwest Laboratories, Richland, WA, 1979.
3. Y. B. Katayama, D. J. Bradley, C. O. Harvey, *Status Report on LWR Spent Fuel IAEA Leach Tests*, PNL-3173, Pacific Northwest Laboratory, 1980.
4. A. D. Mitchell, J. H. Goode, V. C. Vaughen, *Leaching of Irradiated Light-Water-Reactor Fuel in a Simulated Post-Accident Environment*, ORNL/TM-7546, Oak Ridge National Laboratory, 1981.
5. OECD LOFT-T-3810, *Postirradiation Examination Data and Analyses for OECD LOFT Fission Product Experiment LP-FP-2*, Volumes 1 & 2, December 1989
6. OECD LOFT-T-3805, *OECD LOFT Fission Product Experiment LP FP-2 Data Report*, May 1987
7. OECD LOFT-T-3808, *Containment Analysis Report for LOFT Experiment LP FP-2*, January 1989
8. OECD LOFT-T-3806, *Experiment Analysis and Summary Report for OECD LOFT Project Fission Product Experiment LP-FP-2*, June 1989
9. A. B. Johnson, Jr., A. L. Pitner, *Surface Area Considerations for Corroding N Reactor Fuel*, PNNL-11174, Battelle Pacific Northwest Laboratories, Richland, WA, June 1996

# **Appendix A**

## **Sampling/Analytical Methods**

# Appendix A

## Sampling/Analytical Methods

This appendix provides a short description of each of the sampling/analytical methods used to determine the concentration of the elements and radionuclides shown in Tables 1 and 2 of the body of this document.

### A-1. Inductively Coupled Plasma Mass Spectrometry (ICP-MS)

An inductively coupled plasma is a plasma that is energized (ionized) by inductively heating the gas with an electrical coil, and contains a sufficient concentration of ions and electrons to make the gas electrically conductive. Even a partially ionized gas in which as little as 1% of the particles are ionized can have the characteristics of a plasma (i.e., response to magnetic fields and high electrical conductivity). The plasmas used in spectrochemical analysis are essentially electrically neutral, with each positive charge on an ion balanced by a free electron. In these plasmas the positive ions are almost all singly charged and there are few negative ions, so there are nearly equal amounts of ions and electrons in each unit volume of plasma.

An inductively coupled plasma (ICP) for spectrometry is sustained in a torch that consists of three concentric tubes, usually made of quartz. The end of this torch is placed inside an induction coil supplied with a radio-frequency electric current. A flow of argon gas is introduced between the two outermost tubes of the torch and an electric spark is applied for a short time to introduce free electrons into the gas stream. These electrons interact with the radio-frequency magnetic field of the induction coil and are accelerated first in one direction, then the other, as the field changes at high frequency. The accelerated electrons collide with argon atoms, and sometimes a collision causes an argon atom to part with one of its electrons. The released electron is in turn accelerated by the rapidly changing magnetic field. The process continues until the rate of release of new electrons in collisions is balanced by the rate of recombination of electrons with argon ions (atoms that have lost an electron). This produces a 'fireball' that consists mostly of argon atoms with a rather small fraction of free electrons and argon ions. The temperature of the plasma is very high, of the order of 10,000 K.

The ICP can be retained in the quartz torch because the flow of gas between the two outermost tubes keeps the plasma away from the walls of the torch. A second flow of argon is usually introduced between the central tube and the intermediate tube to keep the plasma away from the end of the central tube. A third flow of gas is introduced into the central tube of the torch. This gas flow passes through the center of the plasma, where it forms a channel that is cooler than the surrounding plasma but still much hotter than a chemical flame. Samples to be analyzed are introduced into this central channel, usually as a mist of liquid formed by passing the liquid sample into a nebulizer.

As a droplet of nebulized sample enters the central channel of the ICP, it evaporates and any solids that were dissolved in the liquid vaporize and then break down into atoms. At the temperatures prevailing in the plasma a significant proportion of the atoms of many chemical elements are ionized, each atom losing its most loosely bound electron to form a singly charged ion.

For coupling to mass spectrometry, the ions from the plasma are extracted through a series of cones into a mass spectrometer. The ions are separated on the basis of their mass-to-charge ratio and a detector receives an ion signal proportional to the concentration.

The concentration of a sample can be determined through calibration with certified reference material such as single or multi-element reference standards. ICP-MS also lends itself to quantitative determinations through isotope dilution, a single point method based on an isotopically enriched standard.

## **A-2. Ion Chromatography**

Ion chromatography is a form of liquid chromatography that uses ion-exchange resins to separate atomic or molecular ions based on their interaction with the eluent (mobile phase) and the column packing (stationary phase). Its greatest utility is for analysis of anions as it provides simultaneous, rapid, sensitive, and selective detection.

An ion chromatograph consists of the same basic components: eluent, pump, injection valve, analytical (separator) column, suppressor, detector and the data system. A pump delivers the mobile phase (eluent) through the chromatographic system. The sample is injected into the system via a loop injector. Typically a guard column precedes a separatory column. Separation of the sample is achieved when the sample components carried by the mobile phase migrate and interact with the stationary phase column. The separated sample is carried from the column to a suppressor. The suppressor chemically reduces the high conductivity eluent background while simultaneously converting the sample components to a form that is more conductive. Following suppression, the sample components are carried to the detector.

The most commonly employed detector in ion chromatography is the conductivity detector. Conductivity detection is based upon the electrical conductivity of an ionic solution as it flows between two oppositely charged electrodes. The presence of ions in the solution allows electrical current to flow between the electrodes, thus completing the circuit. At low ionic concentrations, conductivity is directly proportional to the concentration of the conductive species in the solution at a given temperature. The total ionic concentration of the solution in the cell, the degree of dissociation, and the solution temperature affects this relationship. The chromatographic signals are recorded and displayed by the data system. Quantitative results are obtained by evaluating peak areas, which are proportional to the analyte concentrations over a wide range.

This method is applicable for the analysis of bromide, chloride, fluoride, nitrate, nitrite, phosphate and sulfate. The method may also be suitable for other anions when acceptable method performance is demonstrated using quality control elements.

## **A-3. Ion Chromatography Separation and Detection by Alpha Spectrometry**

Ion chromatography separation can be used in conjunction with alpha spectrometry. Alpha spectrometry can be described as recording the energy of the emitted alpha particles in the form of a pulse height distribution. The pulses are created in a sensitive detector volume which can be gaseous, liquid or solid, and registered after electronic amplification. Although the alpha radiation exhibits discrete energies, the interaction between alpha particle and detector is subjected to statistical variations which cause the emergence of a broadened peak instead of a discrete line. Commonly used detector types are ionization chambers, proportional counters, semi-conductors, and scintillation counters. The energy of alpha particles emitted by the known radionuclide ranges in a narrow region of 4 to 9 MeV. Hence, spectrometers with a high energy resolution are required for the analysis of mixtures of alpha emitting radionuclides.

## **A-4. Liquid Scintillation**

Liquid scintillation counting is a standard laboratory method for measuring radiation from beta-emitting radioactive isotopes. Samples are dissolved or suspended in a "cocktail" containing a solvent, typically some form of a surfactant, and small amounts of other additives known as fluors or scintillators. Scintillators can be divided into primary and secondary phosphors, differing in their luminescence properties. An aliquot of the distillate is mixed with scintillation cocktail, allowed to dark adapt in the scintillation counter, and counted for an appropriate time to achieve the desired counting statistics. Smear samples are measured directly without treatment by mixing with water and the scintillation cocktail.

## **A-5. Extraction Fluorophotometric Determination**

This method for detecting uranium, highly selective and sensitive to nanogram levels, is applicable to a wide variety of aqueous and organic samples including plant processing streams that contain high levels of fission products. Its only undesirable feature is limited precision.

Uranium in aqueous samples is separated by extraction as uranyl nitrate into methyl isobutyl ketone from an acid deficient aluminum nitrate salting solution. Solid samples are fused with potassium pyrosulfate, dissolved in dilute nitric acid and then extracted. Organic samples are analyzed directly. The organic phase is evaporated on a sodium fluoride lithium fluoride pellet which then is fused on a burner. The pellet, after cooling, is irradiated with ultraviolet light at 365 nm from a mercury lamp and the resulting fluorescence, which is proportional to the amount of uranium, is measured at 555 nm.

## **A-6. Gamma Spectroscopy**

Gamma-ray spectroscopy is the quantitative study of the energy spectra of gamma-ray sources, in the nuclear laboratory and nuclear process, and other radiation measurement contexts. Most radioactive sources produce gamma rays of various energies and intensities. When these emissions are collected and analyzed with a gamma-ray spectroscopy system, a gamma-ray energy spectrum can be produced. A detailed analysis of this spectrum is typically used to determine the identity and quantity of gamma emitters present in the source. The gamma spectrum is characteristic of the gamma-emitting nuclides contained in the source.